SERI/TR-252-2103
UC Category: 59a
DE84013048

SERI/TR--252-2103

DE84 013048

Heat-Transfer Enhancement in Natural Convection Enclosure Flow

Mark Bohn
Ren Anderson

August 1984

DISCLAIMER

Prepared under Task No. 3735.10
FTP No. 468

Solar Energy Research Institute
A Division of Midwest Research Institute

1617 Cole Boulevard
Golden, Colorado 80401

Prepared for the
U.S. Department of Energy
Contract No. DE-AC02-83CH10093

PREFACE

This report documents research performed under Task Number 1538.10, Convection Enhancement, during FY 1983. The research supports the Passive Technology Program by quantifying the ability of modified building interior surfaces to increase heat transfer from the surface and by quantifying the effect of real surface geometries, obstructions, etc. to affect the heat transfer. The detailed reviews of this report provided by Richard Loehrke, Colorado State University, O. A. Plumb, Washington State University, and Kenjiro Yamaguchi, Los Alamos National Laboratory, are gratefully acknowledged.

Mark Bohn

Ren Anderson

D. Johnson, Acting Chief
Thermal Research Branch

L. J. Shannon, Director
Solar Heat Research Division

SUMMARY

Objective

To determine if a roughened vertical surface comprising one wall of an enclosure exhibits larger natural convection heat transfer than does a smooth surface under conditions simulating the interior of a passively heated building.

Discussion

A dominant mode of heat transfer in passively heated buildings is natural convection from vertical direct gain surfaces. This mode of heat transfer is also very important in determining the performance of storage walls. Previous research demonstrated that the heat transfer mechanism for this mode is laminar boundary layers which flow up heated surfaces transferring heat from the surface and transporting it to cool parts of the building. Since typical buildings operate in the near-transition regime, a logical question is whether the surface heat transfer could not be increased by promoting transition of the boundary layer into turbulent flow. Also of interest is whether a turbulent boundary layer heat transfer could be enhanced. The purpose of this report is to describe literature on this topic and to describe an experimental effort aimed at determining if surface texture modification can be used to increase the heat transfer.

The experimental effort involved testing in a water-filled enclosure in which one vertical surface was cooled and the facing vertical surface was heated--all other surfaces being adiabatic. The heated surface was replaceable in such a way that either a smooth or roughened surface could be tested. The roughness element height was approximately equal to the velocity boundary layer thickness. Average and local heat transfer coefficients were measured and flow visualization was used to depict the point of transition to turbulent flow.

Conclusions

For an isothermal heated surface, the rough texture produced fully turbulent behavior at overall Rayleigh numbers about half that of a smooth surface. This resulted in increases in local heat transfer of about 40% and in the surface average heat transfer of about 16%. The constant flux boundary condition did not exhibit early transition primarily because the experimental apparatus was not capable of achieving sufficiently high Rayleigh numbers.

TABLE OF CONTENTS

		Page
1.0	Heat Transfer Enhancement	1
2.0	Mechanisms of Heat Transfer Enhancement	4
2.1	Surface Roughness	4
2.2	Previous Research on Natural Convection Enhancement	9
2.3	Relationship to Enclosure Flows and Building Interiors	13
2.4	Objective	15
3.0	Testing the Roughened Surface	16
3.1	Procedures and Experimental Errors	19
3.2	Flow Visualization	20
4.0	Results and Discussion	22
5.0	Conclusions and Recommendations	29
6.0	References	31
Appendix A:	Boundary Layer Equations	33

LIST OF FIGURES

		Page
1-1	Examples of Roughened Surfaces for Heat Transfer Enhancement.....	3
2-1	Heat Transfer and Friction Characteristics.....	7
2-2	Predicted Streamline Distribution for Turbulence Promoters in Laminar Channel Flow.....	8
2-3	Local Sherwood Number Distribution between Promoters.....	9
3-1	Cubical Test Cell for Enhancement Experiments.....	16
3-2	Machined Surface for Heat Transfer Enhancement.....	17
4-1	Average Nusselt Number for Isothermal Heated Plate.....	22
4-2	Average Nusselt Number for Constant Heat Flux Heated Plate.....	23
4-3	Flow Visualization.....	24
4-4	Local Heat Transfer Data.....	28
A-1	Solution of the Blasius Problem.....	33
A-2	Velocity Profile for Turbulent Flow over a Flat Plate.....	35
A-3	Velocity Profile for Laminar Natural Convection up a Vertical Heated Plate.....	36

LIST OF TABLES

		Page
3-1	Laminar Boundary Layer Thickness at $Ra_L = 10^{10}$, Pr = 4.5	19
3-2	Experimental Error	20

NOMENCLATURE

A	heat transfer surface area (m^2)
C_p	specific heat (J/kg K)
D	pipe diameter (m)
f	friction factor or a function
G	mass velocity (kg/m^2 s)
g	acceleration of gravity (m/s^2)
Gr_L	overall Grashof number = $g\beta\Delta TL^3/\nu^2$
Gr_x	local Grashof number = $g\beta\Delta Tx^3/\nu^2$
H	height of enclosure (m)
h	heat transfer coefficient (W/m^2 K)
k	thermal conductivity (W/m K)
k_{adm}	admissable roughness height (Eq. 2-3) (mm)
k_{crit}	critical roughness height (Eq. 2-4) (mm)
k_s	height of sand-grain roughness (mm)
L	length scale, height of vertical plate (m)
Nu_x	local Nusselt number = hx/k
$\overline{Nu}_L$	average Nusselt number = hL/k
Pr	Prandtl number = $\mu C_p/k$
Q	rate of heat transfer (W)
R	pipe radius (m)
Ra_L, Ra	overall Rayleigh number = $g\beta\Delta TL^3Pr/\nu^2$
Ra_*	modified Rayleigh number (Eq. 3-4)
Re	average Reynolds number UD/ν
Re_x	local Reynolds number = $U_\infty x/\nu$
St	Stanton number = h/GC_p
T	temperature (K)
u	local average velocity (m/s)
U_o	overall heat transfer conductance (W/m^2 K)
U_∞	free stream velocity (m/s)
u_*	friction velocity (m/s)
U_{max}	maximum velocity in natural convection boundary layer (m/s)
v_*	friction velocity (m/s)
x	distance parallel to a surface (m)
y	distance normal to a surface (m)

NOMENCLATURE (Concluded)

Greek

α	integral defined in Eq. A-7
β	coefficient of thermal expansion (K^{-1})
δ	boundary layer thickness (m)
ΔT_{LM}	log mean temperature difference (K)
ε_s	sand grain roughness height (mm)
ε	roughness height (mm)
ν	kinematic viscosity (m^2/s)
μ	dynamic viscosity (kg/ms)
ρ	density (kg/m^3)
τ_o	wall shear stress (kPa)

Subscripts

b	bulk
c	cold wall
crit	location of transition
h	heated wall
w	wall
x,crit	location of transition to turbulence
∞,crit	ambient conditions at transition
∞,o	ambient conditions at bottom of heated cylinder
∞	ambient
o	wall

SECTION 1.0

HEAT TRANSFER ENHANCEMENT

Heat transfer enhancement is the practice of increasing heat transfer coefficients, providing more heat transfer surface area, or both. Practical embodiments of heat transfer enhancement include surface roughness, turbulence promoters, and fins. Heat transfer enhancement may also be brought about by surface or fluid vibration, electrostatic fields, mechanical aids, etc. These latter methods are called active enhancement techniques because they require external power as opposed to surface treatments, which are called passive enhancement techniques. Heat transfer enhancement may be applied to typical heat exchange equipment for one of the following reasons: (1) to reduce the required heat transfer surface area and, therefore, lower the heat exchanger size and cost, (2) to increase the heat duty of the exchanger for all other parameters being fixed, (3) to permit closer approach temperatures, and (4) to permit lower pumping power and, therefore, reduce operating costs. All of these can be easily visualized from the expression for heat duty for a heat exchanger:

$$Q = U_o \, A \, \Delta T_{LM} \, . \qquad (1\text{-}1)$$

An enhancement technique that only increases the heat transfer coefficient also increases the overall conductance U_o. Therefore, one may either reduce the heat transfer area A, increase the heat duty Q, or decrease the temperature difference ΔT_{LM} for fixed Q and ΔT_{LM}, A and ΔT_{LM}, or Q and A, respectively. In forced convection lower pumping power can be achieved because if the surface heat transfer coefficient is increased by some means, a reduction in the fluid flow velocity over that surface can reduce the heat transfer coefficient to the original value, but the lower flow velocity yields lower pumping costs.

In any practical application, a complete analysis is required to determine the economic benefit of enhancement. Such an analysis must include a possible increased first cost because of the enhancement, increased heat exchanger heat transfer performance, the effect on operating costs (especially a potential increase in pumping power because of roughness, turbulence promotors, and swirl devices) and maintenance costs, etc. A major practical concern in industrial applications is the increased fouling of the heat exchange surface caused by the enhancement. Fouling can quickly eliminate any increase in the heat transfer coefficient because of the enhancement.

There is a very large, rapidly growing body of literature on the subject of heat transfer enhancement. Webb and Bergles (1983) report 2780 papers and reports as of mid-1982 and over 500 U.S. patents related to the technology. Bergles and co-workers at Iowa State University, Ames, have logged the technical articles into a computerized information retrieval system that classifies each document according to the type of flow treated (single-phase natural convection, single-phase forced convection, pool boiling, flow boiling, condensation, etc.) and type of enhancement (rough surface, extended surface, displaced enhancement devices, swirl flow, fluid additives, vibration, etc.).

References to natural convection enhancement number 177 with the majority of those papers dealing with vibration effects. Thirteen papers deal with enhancement of natural convection by extended surfaces and six papers deal with enhancement of natural convection by surface roughness. These two techniques have the most relevance to building applications. Extended surfaces refer to surface projections such as fins where the primary objective is to increase the surface area for heat transfer. This type of heat transfer enhancement is available commercially in the form of ribbed concrete block. It is possible to calculate the performance of most of the finned surfaces because several correlations are available for predicting the heat transfer from such surfaces since they are widely used in natural cooling of electronic equipment.

Surface roughness can include any of several roughness elements that generally do not provide a substantial increase in surface area but, rather, increase the heat transfer coefficient by modifying fluid flow in the boundary layer. Examples of roughness elements include random close-packed sand-grain elements, regularly spaced geometric protuberences, such as pyramids, cylinders, and rectangles (three dimensional), or repeated ribs of various cross section. Figure 1-1 shows examples of some surface roughness elements. Heat transfer behavior of the roughened surfaces is not easily predicted; therefore, this report concentrates on that type of enhancement rather than extended surface enhancement.

The application of natural convection, heat transfer enhancement for passive building applications can provide significantly improved coupling into thermal storage (Neeper and McFarland 1982). If the surface heat transfer coefficient could be doubled, the very large energy storage capacity of phase-change materials could be used to increase the Solar Savings Fraction from 62% to about 90% for the example studied by Neeper. For more conventional sensible heat storage walls, increasing the surface heat transfer coefficient would allow smaller storage walls; storage walls operating at lower temperature, thus reducing thermal losses; or higher rates of heat transfer from the wall. The ability to increase the convective heat transfer from one side of a wall relative to the other side could provide control in the heat flow. For example, heat flow from a direct gain wall on the north side of a sunspace could be increased in the living-space side and decreased on the sunspace side.

An earlier report describes the importance of boundary layers in transferring heat from building interior surfaces (Bohn et al. 1983). More general than just the enhancement effect, then, is the effect of typical surface roughness elements on this boundary layer and, hence, upon heat transfer and air flow in a building. Architectural elements that incorporate surface roughness are in use today, but we cannot presently predict how the surface affects heat transfer. Moreover, typical architectural practice includes elements such as window sills and mullions that could affect the boundary layer flow.

A general objective of this report is to provide a basic understanding of how natural convection boundary layers are affected by surface roughness elements. A particular objective is to focus on the heat transfer enhancement effect of one type of surface roughness.

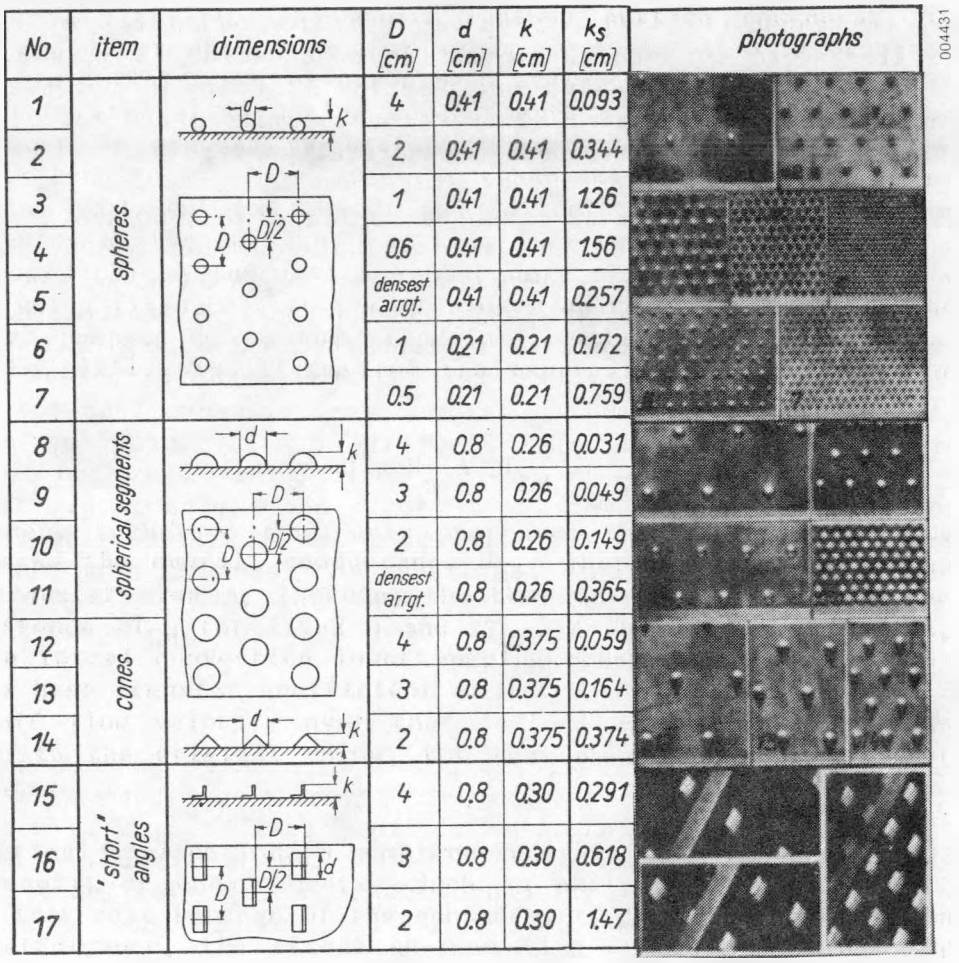

No	item	D [cm]	d [cm]	k [cm]	k_S [cm]
1	spheres	4	0.41	0.41	0.093
2		2	0.41	0.41	0.344
3		1	0.41	0.41	1.26
4		0.6	0.41	0.41	1.56
5		densest arrgt.	0.41	0.41	0.257
6		1	0.21	0.21	0.172
7		0.5	0.21	0.21	0.759
8	spherical segments	4	0.8	0.26	0.031
9		3	0.8	0.26	0.049
10		2	0.8	0.26	0.149
11		densest arrgt.	0.8	0.26	0.365
12	cones	4	0.8	0.375	0.059
13		3	0.8	0.375	0.164
14		2	0.8	0.375	0.374
15	'short' angles	4	0.8	0.30	0.291
16		3	0.8	0.30	0.618
17		2	0.8	0.30	1.47

Figure 1-1. Examples of Roughened Surfaces for Heat Transfer Enhancement
Source: Schlicting (1968)

It is clearly not possible to provide a comprehensive review of enhancement literature in this report, nor is it necessary since some of the previously cited references provide adequate information on recent developments and a good starting point for a literature review. In Section 2.0 we review some of the literature that will give us a background for understanding how heat transfer enhancement occurs. Such a background is necessary to speculate on the mechanisms of heat transfer enhancement in natural convection. Section 3.0 describes an experiment in which the effect of surface roughness on one vertical wall of an enclosure was tested. Section 4.0 presents and discusses the experimental results. Section 5.0 presents conclusions based on the research, and makes recommendations for future research.

SECTION 2.0

MECHANISMS OF HEAT TRANSFER ENHANCEMENT

A majority of the recent review literature (Webb and Bergles 1983; Webb 1980; Nakayama 1982; Bergles 1978) adequately describes recent developments in the technology but generally does not delve into the mechanisms of enhancement. Since the literature on natural convection enhancement is very limited (and tends to be self contradictory, see Section 2.2) it is necessary to rely heavily on the work in forced flow over rough surfaces and forced convection enhancement to understand how to enhance natural convection.

In turbulent flow it appears that the mechanism of heat transfer enhancement is by generating turbulent eddies within the viscous sublayer*. For a smooth surface the viscous sublayer provides a large resistance to heat flow since the heat flow across this layer is by conduction. By generating eddies on this conduction layer, the roughness elements promote mixing of the fluid and, therefore, convective transport of heat to the outer turbulent flow. The penalty for this increased mixing is increased pressure drop (pipe flow) or increased drag (flat-plate flow). Since the driving force for natural flow (bouyancy) is not provided by an external source, this increased drag does not result in increased pumping work as it would for a pipe flow. The increase drag caused by the roughness must, however, act as a retarding force to the bouyant driving force. How this influences heat transfer from the surface is not clear.

2.1 SURFACE ROUGHNESS

To produce any increase in friction, and presumably an increase in heat transfer, the roughness elements must protrude up through the viscous sublayer. A surface with roughness elements small enough to not result in increased friction is known as a hydraulically smooth surface. Roughness elements large enough to produce friction factors in pipe flow independent of the Reynolds number produce what is called fully rough flow. The transition regime falls in between the hydraulically smooth and fully rough regimes. Schlicting (1968) relates the boundaries of the three regimes to the ratio of the roughness element height k_s and the viscous sublayer thickness ν/v_*:

$$\begin{aligned} &\text{Hydraulically smooth} && 0 \leqslant k_s v_*/\nu \leqslant 5 \\ &\text{Transition} && 5 \leqslant k_s v_*/\nu \leqslant 70 \\ &\text{Fully rough} && 70 \leqslant k_s v_*/\nu \ . \end{aligned} \qquad (2\text{-}1)$$

In the hydraulically smooth regime, the roughness elements are all within the viscous sublayer. Immersion of the elements in this viscous flow does not produce additional drag. In the transition regime, the elements protrude part

*For a discussion of boundary layer fundamentals pertinent to Section 2.0, see Appendix A.

way through the viscous sublayer and additional friction is due to form drag on the element. In the fully rough regime, all elements protrude from the sublayer, and since the elements are bluff objects, their drag force follows a quadratic relationship with flow velocity; i.e., the friction is independent of Reynolds number. For pipe flow the friction coefficient is given by

$$f = \left[2 \log(R/k_s) + 1.74\right]^{-2} . \qquad (2\text{-}2)$$

For roughness elements other than sand-grain types, an equivalent roughness height is defined that gives the correct friction coefficient when inserted into Eq. 2-2.

For flow over a flat plate at zero angle of incidence Eq. 2-1 is also valid, although Schlicting (1968) gives a more physically understandable relationship in

$$U_\infty \, k_{adm}/\nu = 100 . \qquad (2\text{-}3)$$

Equation 2-3 gives the admissable height (k_{adm}) of a roughness element, which is the maximum height of an individual element, which does not increase the drag relative to a smooth wall. Equation 2-3 is nearly equivalent to the definition of a fully rough regime, Eq. 2-1, the difference being in the constant 100 in Eq. 2-3 versus 70 in Eq. 2-1.

For laminar flow at very low Re, the protuberance has no effect on the flow since the streamlines follow the surface contours of the protuberance. At higher Re, a stagnant zone forms downstream of the protuberance, and the resulting flow acceleration can increase the local heat transfer. If the protuberance is large enough, it can trip the boundary layer into turbulent flow. The size of the roughness element required to trip the boundary layer depends on the stability, i.e., Re_x, of the boundary layer. Obviously, a boundary layer approaching transition can be tripped by a very small disturbance. Schlicting (1968) gives a criterion for critical height of a cylindrical roughness element needed to cause transition of the element itself:

$$v_* \, k_{crit}/\nu = 15 . \qquad (2\text{-}4)$$

Generally, a much larger roughness element is required to trip a stable laminar boundary layer than is required to produce fully rough flow for a turbulent boundary layer. The constant in Eq. 2-4 increases for grooves and decreases if the tripping wire has a sharp cross section.

One of the earlier studies of the effect of roughness on forced convection heat transfer and pressure drop in the turbulent regime is that of Dipprey and Sabersky (1963). Their results have been cast into an especially convenient form by Webb (1979). Figure 2-1 shows the Stanton number, St, and friction factor as a function of tube Reynolds number at Pr = 5.1 for four values of roughness height-to-tube-diameter ratio. In the fully rough regime the friction factor is only a function of roughness height ε/D. The St reaches a maximum value just before the beginning of the fully rough regime. Picking the maximum value of St for each roughness height, we see that relative to St for the smooth tube at the same Re, heat transfer increases of very nearly two times are possible for the sand-grain roughness. The corresponding friction factor's increase is 1.96 for the roughest tube to 1.54 for the smoothest tube. The Dipprey and Sabersky (1963) data show that as the Pr increases, the

St relative to the smooth tube data increases; i.e., more heat transfer enhancement results for high Pr fluids. We also note that in the fully rough regime all roughness heights produce the same increase in St relative to the smooth tube. Since all roughness elements in this regime extend beyond the viscous sublayer, it is clear that the enhancement effect is not simply caused by an increase in tube surface area provided by the roughness elements. If this were the case the rougher surfaces, with more surface area, would show larger St in the fully rough regime than smooth surfaces.

Based on the relative thicknesses of thermal and velocity boundary layers for high and low Pr fluids, one may conjecture as to the reason for more enhancement in high Pr fluids. For such fluids the thermal boundary layer is much thinner than the velocity boundary layer. A roughness element extending out from the viscous sublayer must therefore extend well into a region of nearly free-stream temperature-fluid. Mixing promoted by the protuberance would be effective because it can bring this fluid, which is near the free stream temperature, into the temperature boundary layer near the wall. A fluid with very low Pr has a much thicker thermal boundary layer than velocity boundary layer. Thus, mixing caused by a surface protuberance would not be able to bring free-stream temperature-fluid into the wall unless the protuberance were much larger than the velocity boundary layer thickness.

Webb (1979) also presents data for roughness elements of the transverse rib type (Figure 2-1b). The general behavior is similar to the sand-grain roughness except that the rib of physical height equal to a sand-grain roughness element produces a larger St and friction factor. For example, a rib height of 0.005 D gives a maximum St relative to the smooth tube St of 2.18, while the friction factor increases by 2.82 relative to the smooth tube at the same Re. Thus, the friction increase is larger with the rib than with the sand-grain roughness. For the rib roughness, Pr has less effect on St than does the sand-grain roughness.

As demonstrated by Lewis (1975), the mechanism of enhancement for repeated ribs (and presumably other roughness shapes) at high Re is the acceleration of flow after a separated recirculating zone that forms on the downstream face of the roughness element. Local heat transfer coefficients at the surface under the recirculating zone are lower than that for a smooth wall, but the increases in local heat transfer coefficient where the flow reattaches downstream of the recirculating zone are large enough to more than compensate (assuming the elements are not so close as to lie in the recirculating zone of the upstream element).

A similar effect was found by Kang and Chang (1982) for laminar channel flow with rib-like protuberances on the walls. In that study, mass transfer coefficients (Sh, Sherwood number) were computed for a two-dimensional channel flow with turbulence promoters fixed to the upper and lower channel walls. Figure 2-2 shows the computed streamline distribution. (Note that flow visualization studies confirmed the predicted streamline pattern qualitatively.) For sufficiently large Re ($\sim$ 50) a separated zone forms downstream of the lower wall protuberence. (At a very low Re, the streamlines would completely fill the channel; i.e., the flow would follow the wall contours.) Slightly higher Re ($\sim$ 100) causes the separated zone to expand and also results in the formation of a second separated recirculating zone upstream of

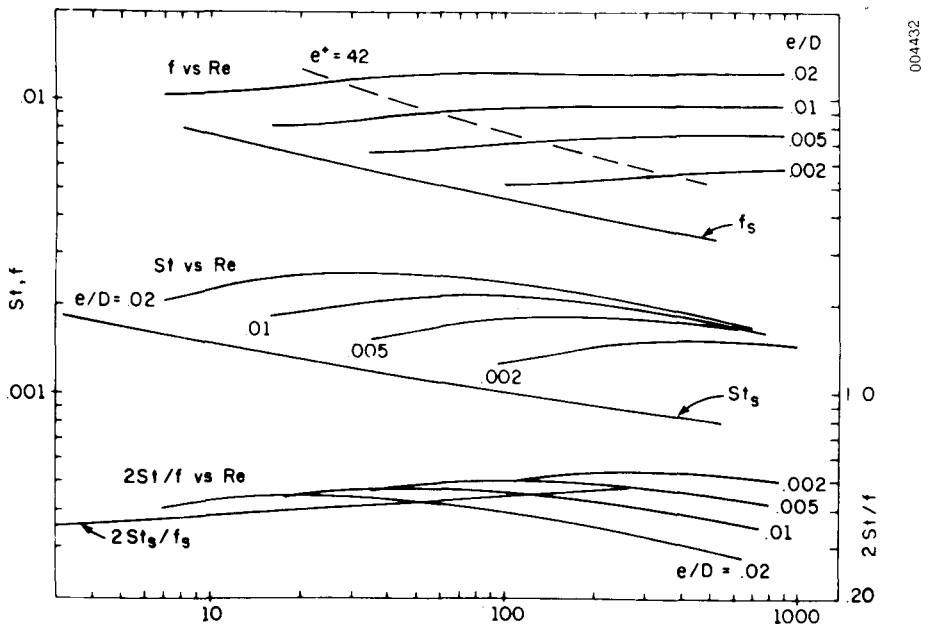

a. Sand-Grain Roughness (Pr = 5.1)

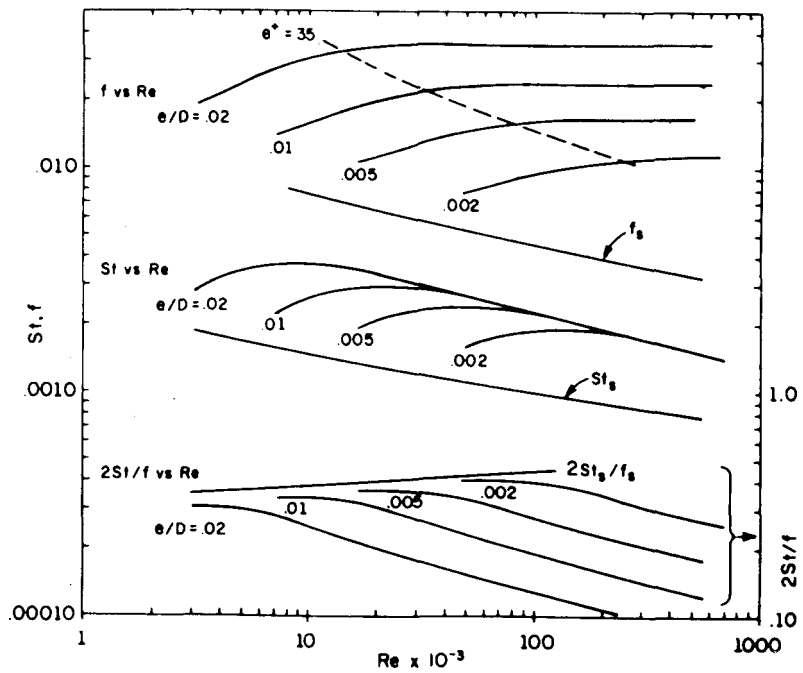

b. Transverse Rib Roughness (Pr = 5.1)

Figure 2-1. Heat Transfer and Friction Characteristics
Source: Webb (1979)

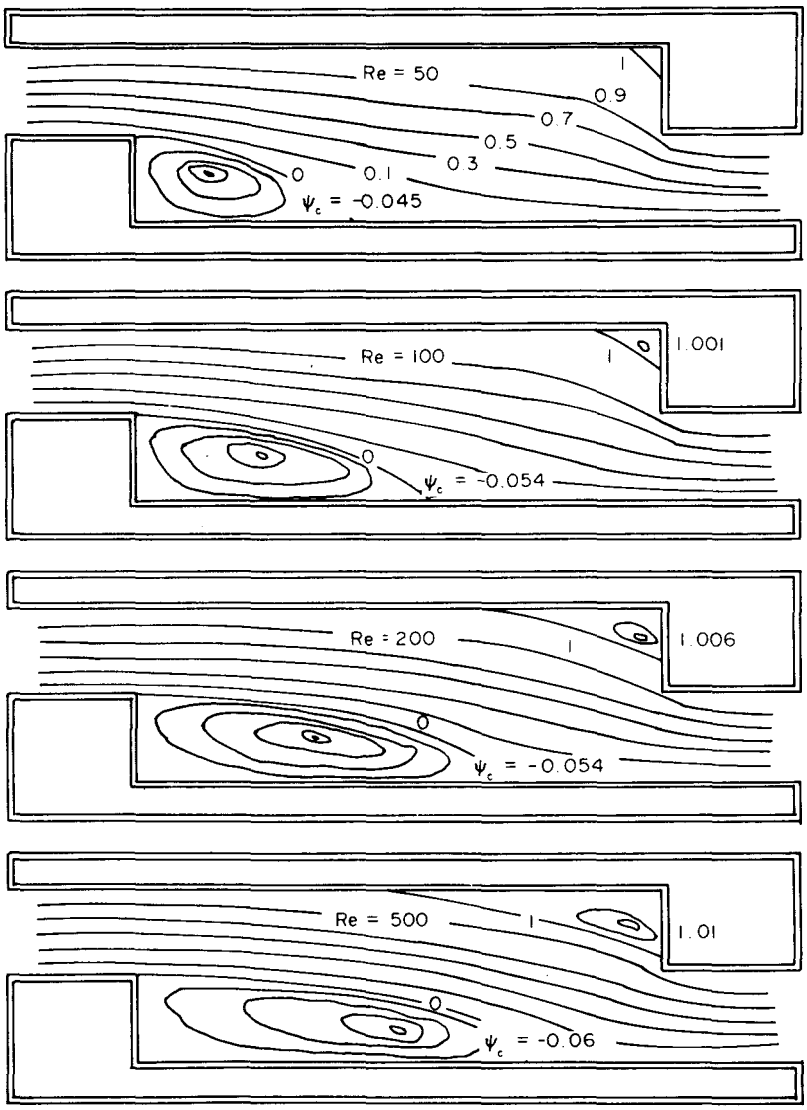

Figure 2-2. Predicted Streamline Distribution for Turbulence Promoters in Laminar Channel Flow
Source: Kang and Chang (1982)

the upper wall protuberance. This zone increases in size with further increases in Re as does the lower separated zone until, at Re ~ 250-300, flow unsteadiness begins and leads to turbulent flow for Re ~ 400.

For the laminar flow regime (Re $\lesssim$ 300) the main fluid stream must flow around the separated zones and in doing so must accelerate, thereby producing increased mass transfer. Figure 2-3 depicts the local Sherwood number Sh_x calculated by Kang and Chang (1982) for both the upper and lower surface. Clearly, the stagnant regions result in very low local mass transfer, although

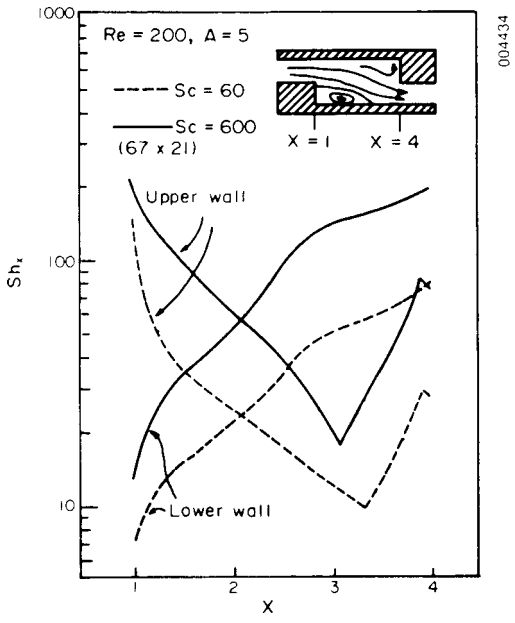

Figure 2-3. Local Sherwood Number Distribution Between Promoters. Source: Kang and Chang (1982)

the accelerated flow beyond these zones gives rise to very large increases in Sh_x. For close enough spacing of the protuberances at large Re one would imagine that the recirculating zones could completely fill the area between protuberances, thereby resulting in low heat transfer. At the other extreme very large spacing would produce very small recirculating zones and accelerating zones, so the average heat transfer coefficient would be very close to that of a smooth wall. Thus, one would expect a certain intermediate protuberance spacing that would give maximum enhancement.

The same arguments should hold true for three-dimensional protuberances, since the separated zone will take the form of a three-dimensional stagnant area attached to the rear of the protuberance. Seban and Caldwell (1968) present data that confirm this. They measured the local heat transfer coefficient on a plane near a sphere attached to the plane. The two spheres tested were 0.64 cm and 1.91 cm in diameter or roughly the boundary layer displacement thickness for the small sphere. The local heat transfer coefficient compared with that for the plate without the sphere is increased slightly ahead of the sphere and is increased significantly behind the sphere. The heat transfer coefficient reaches a maximum approximately two diameters downstream of the sphere where the separated flow reattaches. The local heat transfer increase is about twice that of the plate without a sphere and remains larger than the plain plate for more than 20 diameters downstream of the sphere. This downstream region of heat transfer enhancement is about four diameters wide in the spanwise dimension. The peak in the local heat transfer distribution was seen to be about 50% larger than that behind a (two-dimensional) backward-facing step. The effect of multiple spheres on the plate was not studied by Seban and Caldwell.

2.2 PREVIOUS RESEARCH ON NATURAL CONVECTION ENHANCEMENT

As mentioned in Section 1.0, there has been very little research in the area of natural convection enhancement. This section reviews that literature to provide a background for the experimental portion of the present work.

Prasolov* (1961) measured heat transfer in natural convection from a horizontal cylinder 10-76 mm in diameter in air with pyramid-shaped roughness elements 0.08-0.36 mm in height. He found that in the range of $3 \times 10^5 < Ra_D < 10^6$, the Nu for the roughened cylinders was about twice that of the smooth cylinders and attributed the enhancement to the effect that the roughness elements had on transition. Note that transition for this geometry normally occurs for $Ra_D \sim 10^9$.

Joffre and Barron (1967) solved the integrated boundary layer equations for a vertical plate in natural convection using a velocity profile like Eq. A-10 and a corresponding temperature profile. Then, making use of the heat and momentum transfer analogy and a friction factor expression for rough plates in parallel forced flow, they developed an expression for the Nusselt number as

$$\overline{Nu} = \frac{0.3643\ Ra_L^{1/2}}{(1.89 + 1.62\ \log L/k_s)^{2.5}\ (1 + 0.525\ Pr^{2/3})^{1/2}\ Pr^{1/6}} \quad . \qquad (2\text{-}5)$$

They also measured the heat transfer from an isothermal vertical plate in air ~0.8 m high with horizontal ribs of triangular cross section, height 0.76 mm and spacing 0.89 mm. The data fell in the transition range $10^9 < Ra_c < 1.5 \times 10^9$ and showed an increase in Nu of about 100% compared with accepted correlations in that regime. They did not test a smooth plate. To get good agreement with Eq. 2-5, it was necessary to assign an equivalent sand-grain roughness height of nearly 21 times the height of the machined grooves. As pointed out in Section 2.1, equivalent sand-grain roughness heights of machined ribs are greater than the actual rib height, but the factor of 21 seems large. The effect beyond transition was not tested.

Fujii et al. (1973) measured the natural convection heat transfer from a vertical cylinder in water and in oil. Three types of roughness elements were tested: closely spaced pyramids, widely spaced horizontal ribs of square cross section, and three-dimensional ribs made by removing portions of the square cross-section ribs. They did not report any change in heat transfer coefficient in either the laminar or turbulent regime for water or oil. Temperature profiles for the repeated rib (0.5-mm rib height, 12.8-mm rib spacing) indicated that near the rib the boundary layer profile was very close to that for the smooth surface, although between ribs, the boundary layer was thickened by the ribs presumably because of separated flow. Close examination of their flow visualization photographs for repeated ribs and water seems to confirm the separated region just above each rib, although the detail in the boundary layer is lacking. The temperature measurement between ribs seems to have been made just after the reattachment point, so the boundary layer thickness has not completely returned to that of a smooth surface. By the time the flow reaches the next rib, the boundary layer has returned to that profile of a smooth surface. The thickening of the boundary layer seems to begin just after the rib.

*This article, originally published in Russian, has been translated to English and is available from the senior author of this report.

It is instructive to compare the roughness element height used by Fujii et al. (1973) with the height required to trip a laminar boundary layer and with the thickness of their viscous sublayer. From Figure A-3 we see that the maximum velocity in the laminar boundary layer for Pr = 10 (water) is

$$\frac{u_{max}}{2\sqrt{gx}} \quad \frac{T_\infty}{T_w - T_\infty} = 0.12 \ . \tag{2-6}$$

Since $$Gr_x = \frac{gx^3}{\nu^2} \frac{T_w - T_\infty}{T_\infty} \ ,$$

we have $$\frac{u_{max} x}{\nu} = 0.24 \ Gr_x^{1/2} \ .$$

Because the free-stream velocity is zero, we use u_{max} from Eq. 2-6 for U_∞ in the Reynolds number to find the local shear stress, Eq. A-2,

$$\tau_o(x) = 0.332 \rho u_{max}^2 \left(\frac{u_{max} x}{\nu}\right)^{-1/2} \ ,$$

which gives

$$u_* = \left(0.332 \ u_{max}^2\right)^{1/2} \left(\nu / u_{max} x\right)^{1/4}$$

for the friction velocity. Equation 2-4 gives the critical height to trip the laminar boundary layer:

$$k_{crit} > 15\nu/u_* \ .$$

Choosing Fujii's data in the laminar regime, $Gr_x = 7.56 \times 10^9$ at x = 32 cm inserted into Eq. 2-6. The equation

$$u_{max} = 20{,}870\nu/x$$

gives for the critical height:

$$k_{crit} = \frac{15\nu}{0.048} \frac{x}{20{,}870\nu} = 0.015x = 0.48 \text{ cm} \ .$$

Therefore, their rib height of 0.5 mm was 10 times too small to trip the laminar boundary layer. As noted before, the rib was large enough to cause what appeared to be a separated region downstream of the rib. Their measurements did not indicate any increase in local heat transfer near the ribs. Their spatial resolution may have been inadequate because such an increase was found by Kang and Chang (1982) as described earlier. Note that the boundary layer thickness for the water experiment at these conditions is (from Figure A-3) about 3.7 mm.

Using Fujii's data in the turbulent regime, we see that $Gr_x = 4.45 \times 10^{13}$ at x = 72 cm with Vliet and Liu's recommendation (see Appendix A) for the friction velocity:

$$\frac{xu_*}{\nu} = Gr_x^{1/2} .$$

We find from Eq. A-5 for the thickness of the viscous sublayer that

$$y = 5\nu/u_* = 5\,\frac{x}{Gr_x^{1/2}} = 5.4 \times 10^{-4}\text{mm} ,$$

which is much smaller than the rib height, 0.5 mm.

In fact, the rib height of 0.5 mm would give

$$\frac{yu_*}{\nu} = \frac{y}{x}\,Gr_x^{1/2} = 4632 ,$$

which suggests that the roughness is approximately 70 times the height required for the fully rough regime (see Eq. 2-1). Now, referring to Figure 2-1b, we recall that with the fully rough regime, the friction factor depends only on roughness height, but St decreases after a maximum (which occurs at decreasing Re for increasing roughness) and does so more rapidly for transverse ribs than for a smooth surface. One can see then that excessively large roughness elements could produce no increase in heat transfer relative to a smooth surface. Fujii's data also reinforce the idea that in the turbulent regime, the increase in surface area due to roughness does not necessarily increase heat transfer.

Sastry et al. (1976) measured heat transfer from a vertical cylinder 32.8 mm in diameter × H = 470-mm height in air with roughness provided by wrapping a wire (0.45, 0.81, 1.02, or 1.45 mm in diameter) around the cylinder with a pitch equal to the wire diameter; i.e., no gap between the wires. For the range $7 \times 10^8 < Gr_H < 4 \times 10^9$ they found that the Nu values for the rough surfaces were consistently 50% greater than the Nu values for the smooth surface tested. Here again it appears that testing was done just below transition and that the roughness elements promoted transition of the boundary layer into turbulence. Note that comparing Sastry's rough tube data with those for smooth vertical cylinders recommended by Kreith (1973), for example, implies an enhancement of significantly less than 50% at the high end of Sastry's data ($Gr = 3.7 \times 10^9$) where a 6% increase is seen; at $Gr = 2.07 \times 10^9$, a 17.6% increase is seen; and at $Gr = 1.17 \times 10^9$, a 41% increase is seen. It seems advisable to use the same experimental apparatus and experimental procedure for both smooth and rough surfaces before comparing rough surface data with data from other sources. This is especially true in the transition regime where results are especially sensitive to geometry.

Heya et al. (1982) studied experimentally the laminar regime for horizontal cylinders, with smooth and rough surfaces, 63 and 35 mm in diameter, and of various heights from 0.15 to 0.72 mm in air and water. Contrary to Prasolov, Heya did not find any increase in Nu for any roughness, cylinder diameter, or for air or water even though his data spanned a relatively large range of $Ra = 4 \times 10^4$ to 8×10^6 for air and $3 \times 10^6 < Ra_D < 2 \times 10^8$ for water. No explanation of the discrepancy with Prasolov's data was given. Note that in this range of Ra, the boundary layers remain laminar over the entire cylinder surface. From Heya's interferogram in air the thermal boundary layer [or since Pr = O(1), the velocity boundary layer] is about 4 mm thick or about 6

times the largest roughness height and 30 times the smallest roughness height. Since the water data for Ra were about 100 times larger, we would expect velocity boundary layers $\sim 100^{-1/4} = 0.32$ times the air values. Heya's values of roughness height to boundary layer thickness for air are similar to Fujii's. Since we were able to show that Fujii's roughness elements were much too small to trip the boundary layer into turbulence, the same conclusion could be drawn about Heya's results. For Heya's water data, Ra_D values were up to 2×10^8 where transition normally occurs near $Ra_D \sim 10^9$. The velocity boundary layers should be about twice the largest roughness height or about 10 times the smallest roughness height. Apparently, the Ra_D was well enough below the transition value so the boundary layer was stable enough to resist tripping by the roughness elements tested. It would appear that had Heya tested closer to transition, some influence of roughness would be seen. It is difficult to imagine a boundary layer on a smooth surface that is unstable because of the approach of transition not being effected by a surface protrusion. This is especially true for the horizontal cylinder where the boundary layer must have a tendency to separate on the back side of the cylinder at sufficiently high Rayleigh number.

Some general comments regarding these previous efforts are in order before proceeding. There appears to be some conflicting results as to whether enhancement of natural convection is possible. In the laminar regime previous attempts have not succeeded, possibly because the roughness elements were too small to trip the boundary layer. One exception is the data of Prasolov, which were well below transition but still gave increases of about two times in the heat transfer coefficient. In the transition regime, enhancement seems more likely, since any type of surface roughness will probably cause the unstable boundary layer to transition to turbulence. In the turbulent regime we have only Fujii's data to rely on, which did not show any enhancement effect, possibly because the roughness elements were much larger than the viscous sublayer. Some of the conflicting results described here may be related to not having tested smooth and rough surfaces but, rather, relying on literature data for comparison purposes.

It seems likely that enhancement of natural convection will be possible for applications in which the flow is normally near transition. Different types of surface roughness should be tried including sand-grain, transverse rib, pyramids, and perhaps, single or isolated boundary layer trip fences. The lower the Rayleigh number of the flow, i.e., small rooms, the more stable the boundary layer and the larger the required disturbance to trip the boundary layer. For high Rayleigh number flows, large rooms, atria, etc., enhancement could involve first tripping the laminar portion of the boundary layer to achieve turbulent flow as early as possible, then enhancing heat transfer by modifying the turbulent boundary layer. That latter step should involve a mechanism for disrupting the viscous sublayer, but past research indicates that either that is not effective or that one must be careful to size (or perhaps shape) the protuberance. If a protuberance much larger than the viscous sublayer does not give increased heat transfer, then this suggests a relationship between the increased friction created by the roughness that must in some way tend to retard the bouyant driving force and the ability of the retarded flow to remove heat from the wall. In other words, it may be possible to disturb the turbulent boundary layer with a very large protuberance in such a way to offset any increase in heat transfer by retarding the flow.

It would seem advisable to test roughness elements in the turbulent regime to cover a wide range of roughness height-to-viscous sublayer thickness ratio.

2.3 RELATIONSHIP TO ENCLOSURE FLOWS AND BUILDING INTERIORS

All the previously described research involved heated objects immersed in an "infinite" body of fluid. The geometry most closely related to a building interior is an enclosure in which the body of fluid is completely contained within the solid boundaries of the enclosure. By imposing different temperatures on the boundaries, natural convection flows are set up in the enclosure. As shown by Bohn et al. (1983), at high Rayleigh numbers ($\sim 10^{10}$) such as one would find in building interiors the flow consists essentially of two-dimensional boundary layers on the vertical walls if the horizontal boundaries are adiabatic. The core tends to stratify and exhibits very low velocities. The wall boundary layers remove heat from warm walls, flow across the top and down cool walls, transferring heat to the cool wall. That work also showed that building interiors operate near the point of boundary layer transition, suggesting the possibility of enhancement by promoting transition.

The two major differences between the enclosed flow and the infinite medium flow are the corner at top and bottom of the enclosure and stratification of the enclosure core. In the enclosure, fluid rising along a warm wall has different initial conditions than if the wall were an isolated vertical plate in an infinite medium. In the latter both the thermal and velocity boundary layers start at the leading (lower) edge of the heated plate. Moreover, the fluid approaching the vertical isolated plate has no component of momentum normal to the plate. In the enclosure, the fluid approaches the vertical wall from the horizontal direction and must turn the corner to flow upward. This fluid flows across the horizontal adiabatic surface driven by inertial forces. Thus, the velocity boundary layer is somewhat developed before it reaches the corner.

As pointed out by Fujii et al. (1979), stratification in the ambient fluid affects transition to turbulent flow. They found that the Ra_x (evaluated at condition far from the wall but at the height x of transition) could be correlated by

$$Ra_{x,crit} = (4\sim 8) \times 10^9 \left[\frac{T_{\infty,crit} - T_{\infty,o}}{(T_o - T_\infty)_{crit} x_{crit}} \right]^{-0.86} , \qquad (2\text{-}7)$$

where $T_{\infty,crit}$ is the ambient fluid temperature at the transition height, $T_{\infty,o}$ is the ambient fluid temperature at the bottom of the enclosure, and $(T_o - T_\infty)_{crit}$ is the temperature difference between the wall and the ambient fluid at $x = x_{crit}$. In Eq. 2-7, the dimension of the quantity in brackets is m^{-1}.

Equation 2-7 states that the transition Rayleigh number based on local conditions at transition decreases as the stratification increases. Although Fujii's work was primarily concerned with the effects of stratification that is inevitable when one places a heated object in a tank of liquid to simulate an infinite medium, it should be applicable to enclosures where stratification

occurs naturally because of very low core velocities. Fujii gave no physical explanation for this effect of stratification on transition. However, one can see that since the bouyant driving force is the temperature difference between the wall and ambient fluid, a modification of the ambient fluid temperature, e.g., stratification, could effect stability. Stratification could explain why most researchers have found transition Ra in enclosures one or two orders of magnitude higher than for an isolated vertical plate, except that Eq. 2-7 unfortunately predicts a decrease in Ra_{crit} for increasing stratification. Equation 2-7 is also suspect in that zero stratification yields infinite $Ra_{x,crit}$. Since stratification could interact with surface roughness to promote turbulence, it should be considered in the future. The best way to account for both stratification and the top/bottom corner is to perform experiments in an enclosure to determine the effect of roughness.

2.4 OBJECTIVE

Based on previous discussions of the literature, it appears likely that the convective heat transfer coefficients found in building interiors can be increased via various heat transfer enhancement techniques. The literature seems somewhat contradictory with some researchers finding increases of 100% and others finding no increases under the same conditions. However, near the transition regime (typical of building interiors) it seems that perturbing the boundary layer should promote turbulence and enhance heat transfer; this is consistent with most of the previous work. Whether stable laminar boundary layers and fully turbulent boundary layers can be enhanced is open to question but certainly deserves a more in-depth study than in the past.

A major objective of the work described here is to determine if surface roughness can promote transition to turbulence in a laminar boundary layer and, if so, what effect this has on heat transfer from the surface.

Since no information is available regarding enhancement of natural convection in an enclosure and since an enclosure flow differs in important ways from the geometries tested, it is important to test a rough surface in an enclosure. If it is possible to promote transition, then it is important to understand how a certain promoter works, i.e., its effect on the boundary layer, so one can determine the best type of enhancement to use.

SECTION 3.0

TESTING THE ROUGHENED SURFACE

Based on previous work on three-dimensional natural convection (Bohn et al. 1983), testing the enhancement concept in a fully three-dimensional enclosure seems unnecessary. That work showed that for the high Rayleigh numbers one encounters in buildings, the boundary layers are thin enough to not be influenced by the side walls except perhaps very close to the side wall. A logical simplification then is to test a roughened surface in a two-dimensional enclosure. This will still retain the core stratification and corner aspects peculiar to enclosures as discussed in Section 2.3.

Figure 3-1 shows the test cell based on the cell used in earlier studies. The cell has been modified to allow testing of a heated, rough vertical surface with a facing, cooled, smooth vertical surface. All remaining walls are adiabatic and smooth. The heated wall has 16 equal area resistance heaters attached to its outside surface and can be operated in the isothermal or constant heat flux mode. The cool wall has milled channels through which cooling water is pumped. The side walls are 1.27-cm lucite to allow for flow visualization studies.

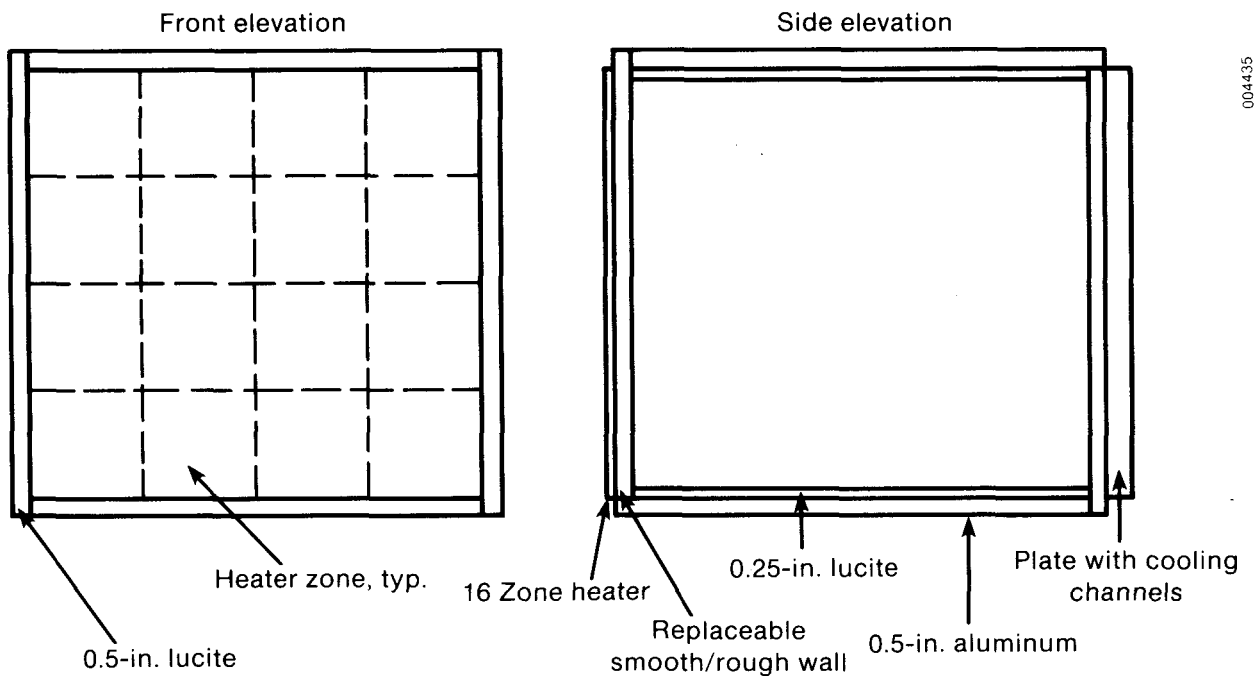

Figure 3-1. Cubical Test Cell for Enhancement Experiments

The height of the test cell interior is 29.2 cm, and this is the length scale used in the dimensionless parameters, Nu, Ra, and Ra_*. The test cell interior width and depth is 30.5 cm.

In this study, a machining operation was used to produce the surface roughness. Referring to Figure 3-2, the surface was produced by milling a set of grooves spanning the plate at 45° from the left of vertical and a similar set at 45° to the right of vertical. The grooves are 1 mm wide, 1 mm deep, on 1-mm centers. Special care was taken to ensure that the edges were clean and free of burrs. These dimensions were chosen to be consistent with the velocity boundary layer thickness. From Figure A-3 the laminar boundary layer

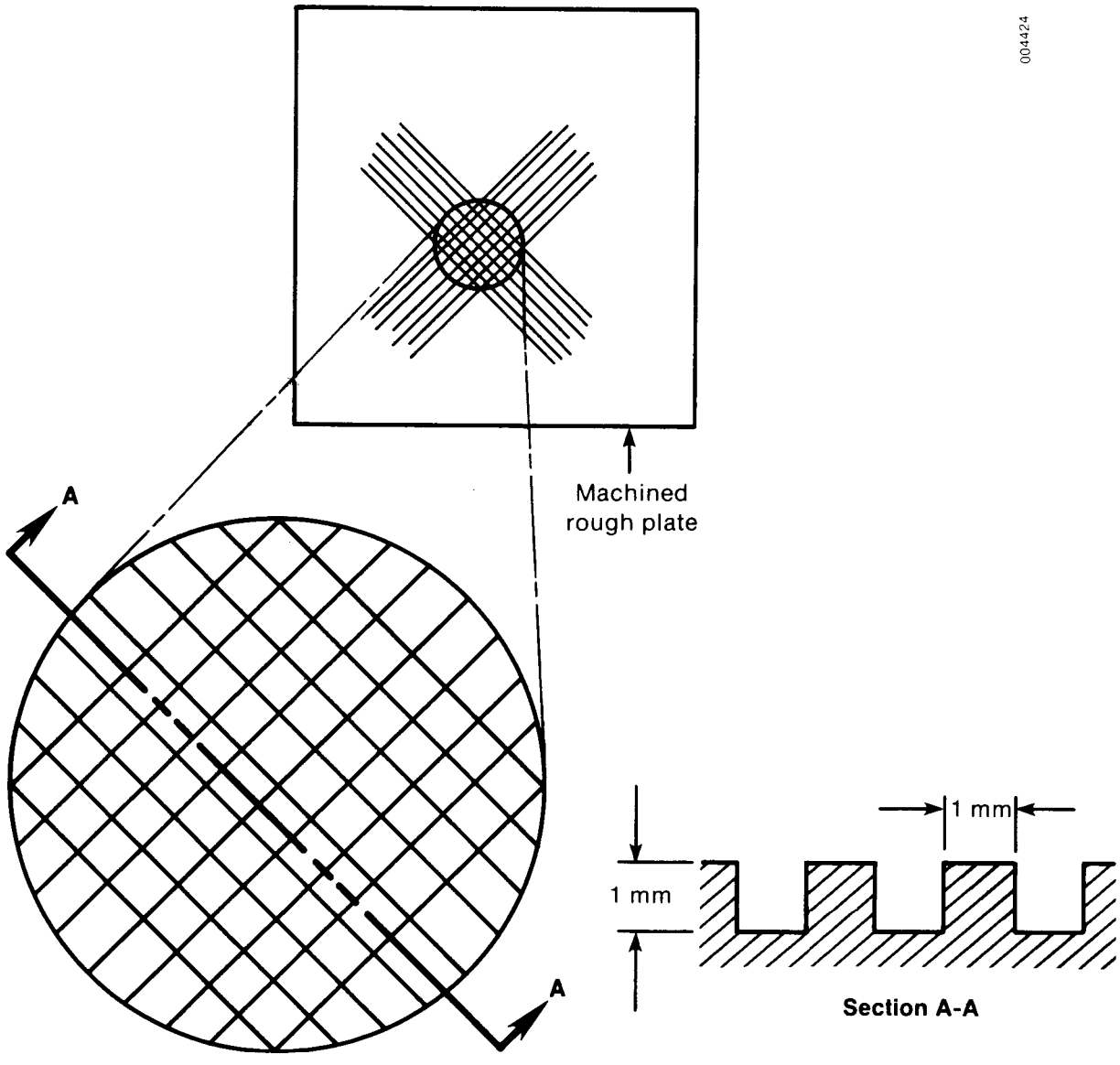

Figure 3-2. Machined Surface for Heat Transfer Enhancement

thickness (taken at the point where the velocity is the peak value) is approximately

$$\delta/x = 0.7\ (Gr_x/4)^{-1/4} \qquad (3\text{-}1)$$

for Pr = 4.5. Since

$$Gr_x = \left(\frac{x}{L}\right)^3 Ra_L/Pr$$

for an isothermal boundary condition, we can calculate the thickness of the boundary layer as a function of height up the heated, smooth plate given the mean Rayleigh number. Note that this is strictly correct for an isolated vertical plate, not an enclosure interior. Table 3-1 gives the results for $Ra = 10^{10}$, typical of the test cell operating conditions.

According to the procedure outlined in Section 2.0, the required height of a cylindrical element to trip this laminar boundary layer may be calculated:

$$\frac{k_{crit}}{x} = \frac{15\nu}{u_* x} = 15\left(\frac{\nu}{u_{max} x}\right)\left(\frac{u_{max}}{u_*}\right) ;$$

from Figure A-3, Pr = 4.5;

$$\frac{u_{max} x}{\nu} = (2)(0.18)Gr_x^{1/2} ;$$

from Eq. A-2:

$$\frac{u_*}{u_{max}} = 0.576\left(u_{max} x/\nu\right)^{-1/4} ,$$

thus

$$\frac{k_{crit}}{x} = (56.0)Gr_x^{-0.375}$$

$$Gr_x = \left(\frac{x}{L}\right)^3 Ra_L\ Pr^{-1} ;$$

at

$$\frac{x}{L} = 0.5,\ Pr = 4.5,\ Ra_L = 10^{10} ,$$

thus

$$k_{crit} = 5.6\ mm . \qquad (3\text{-}2)$$

Therefore, the roughness elements used here at 1-mm height are about the same as the boundary layer thickness and about 1/5 the height of a single, cylindrical element needed to trip the boundary layer.

Note that in designing the roughness, there are several uncertainties. As discussed previously, because the boundary layer approaches the heated surface normally and perhaps is somewhat developed, it differs from conditions used to derive the boundary layer equations regarding tripping. Also, stratification could affect the stability of the boundary layer. Certainly, using characteristics of the laminar, natural convection boundary layer (u_{max} in place of U_∞)

Table 3-1. Laminar Boundary Layer Thickness at $Ra_L = 10^{10}$, Pr = 4.5

x (cm)	x/L	δ (mm)
2.92	0.1	0.75
5.84	0.2	0.90
11.68	0.4	1.07
17.52	0.6	1.18
23.36	0.8	1.27
29.2	1.0	1.33

to derive the required trip height is suspect. Moreover, there are many types of roughness elements one could test. Perhaps the outstanding features of the roughness depicted in Figure 3-2 are that it was reasonably easy to machine, is reproducible, seems to have sufficient roughness height to trip the boundary layer, and will be easily modified for future testing of alternative roughness configurations.

3.1 PROCEDURES AND EXPERIMENTAL ERRORS

The heated vertical surfaces could be replaced to allow testing with the rough surface or with a smooth surface. In this way, a direct comparison could be made, rather than relying on previous data, which seems to be the case in much of the literature.

Given the temperature of the heated plate for isothermal operation T_h and the temperature of the cooled plate T_c, the data are expressed in dimensionless form as

$$\overline{Nu} = \frac{Q}{A(T_h - T_c)} \frac{H}{k} \tag{3-3}$$

and

$$Ra = \frac{g\beta(T_h - T_c)\, H^3}{\nu^2} Pr,$$

where the fluid properties, k, β, Pr, and ν are evaluated at $T_b \equiv (T_h + T_c)/2$. The heat transfer area A is 29.2 × 30.5 = 890.6 cm^2, and no allowance was made in A for the increase caused by roughness.

For the constant flux boundary condition it is necessary to modify the definition of the Rayleigh number to

$$Ra_* = \frac{H^4 g\beta(Q/A)}{\nu^2 k} = RaNu \tag{3-4}$$

because the temperature difference varies over the plate, although the heat flux Q/A is constant.

Generally, the cool plate average temperature T_c was 21 ±2°C. Variations in Ra were achieved by increasing T_h in the range 34°C to 75°C. Variations in Ra_* were achieved by increasing the heat flux from 0.18 to 1.41 W/cm^2.

The cooled wall was held isothermal within ±4% of the overall temperature difference. In the isothermal mode, the temperature variation across the heated plate was less than ±0.4°C. This was achieved by computer control over the 16 independent heaters. The algorithm was a proportional, integral, differential control scheme. Radiation heat transfer was negligible because of the relatively low wall temperatures, relatively large convection heat transfer coefficients, and a nickel electroplating on the heated and cooled surface that gave an infrared emissivity of 0.05. Conduction losses through the neoprene gaskets and through insulation external to the test cell were calibrated at 1.1 W/°C overall temperature differential. This conduction loss was accounted for in the actual wall heat transfer measurement.

The major sources of experimental error were the measurement of the power dissipation Q and the temperature of the heated plate. Because of the control scheme used to turn the 16 heaters on and off, the average power never became totally steady. Errors in computing Q because of this oscillation were approximately ±2% of the indicated value. Although the cooled wall could be held isothermal no better than ±4% of the overall temperature difference, this error is systematic since it was consistent for both tests with the rough plate and the smooth plate. Oscillations in T_h of ±0.4°C were random and do contribute to uncertainty in measuring Ra and Nu for the rough and smooth tests. This error in T_h produces an error in $T_h - T_c$ of approximately 2%. As shown in Table 3-2 the error in Q and $T_h - T_c$ gives an uncertainty in Ra and Ra_* of ±2% and in Nu of ±3%. Therefore, we may consider differences in Nu between the rough and smooth surface to be significant if they are larger than 3%.

Table 3-2. Experimental Error

Q	$T_h - T_c$	Ra	Ra_*	Nu
±2%	±2%	±2%	±2%	±3%

3.2 FLOW VISUALIZATION

For purposes of interpreting the heat transfer data, it is instructive to be able to visualize the important features of the natural convection flow. In the present case, the most important feature is the boundary layer on the heated, vertical wall. The temperature gradient across the boundary layer makes feasible any of several candidate visualization techniques. The method we have chosen here is the mirage method first described by Fujii et al. (1970).

This method uses the index-of-refraction gradient in the boundary layer that results from the temperature gradient. Since the temperature in the boundary layer decreases with distance from the heated wall, the index of refraction increases with distance from the wall. Therefore, light rays passing through

the boundary layer are refracted towards the wall. If an object is placed on one side of the test cell and viewed from the other side, the image will be distorted. This is because portions of the object near enough to the wall to be in the boundary layer appear farther from the wall than they actually are.

For visualizing the boundary layer in the present experiments, an especially convenient object is a series of closely spaced vertical lines parallel to the wall. Because of the temperature gradient near the wall, the lines close to the wall appear displaced away from the wall, while those farther from the wall at the same height remain parallel. This is strictly true only for a laminar boundary layer where the image will be steady and only displaced normal to the wall. In the turbulent portions of the boundary layer the flow is unsteady, three-dimensional, and random. The image of the lines will appear chaotic in the turbulent boundary layer. For this reason the mirage method is especially useful for observing boundary layer transition.

The vertical lines used in Figure 4-3 were drawn with a size 1 Rapidograph pen on 1 mm centers. A total of 17 lines were drawn producing a band of 16 mm total width. Index lines were drawn every 1 cm of vertical distance. The grid was lit from the back with a photographic floodlamp and photographed with a 4×5 camera with a Polaroid back on Type 52 film and on 35-mm Tri-X film.

SECTION 4.0

RESULTS AND DISCUSSION

Average Nusselt numbers are shown in Figures 4-1 and 4-2 for the isothermal and constant heat flux modes, respectively. For the isothermal mode the laminar, transition, and turbulent regimes are delineated. Deviation of the rough surface data from the expected laminar behavior($Nu \sim Ra^{1/4}$) to the turbulent behavior ($Nu \sim Ra^{1/3}$) begins at $Ra = 2 \times 10^{10}$ and ends at $Ra = 2.5 \times 10^{10}$. For the smooth surface this transition begins at $Ra = 3.2 \times 10^{10}$ and is complete near $Ra = 5 \times 10^{10}$. (The regime marked transition refers to the total range over which both surfaces are undergoing transition.) It is clear from Figure 4-1 that the roughened surface does promote transition to turbulence because what appears to be fully turbulent behavior occurs at a Rayleigh number about half that of the smooth surface, $Ra = 2.5 \times 10^{10}$ vs. $Ra = 5 \times 10^{10}$.

In the laminar regime there appears to be no enhancement effect; the rough data and smooth data are within experimental error. In the turbulent regime there appears to be a slight enhancement effect, since the rough data lie approximately 4% above the smooth data. The largest increase is in the transition regime, where because of early transition the rough data are as much as 16% above the smooth data. From Eq. 3-2 we saw that a single cylindrical roughness element would need to be about 5 mm high to cause transition at the element. Apparently, the roughness elements used here are much more effective than a cylindrical element since they are only 1 mm high.

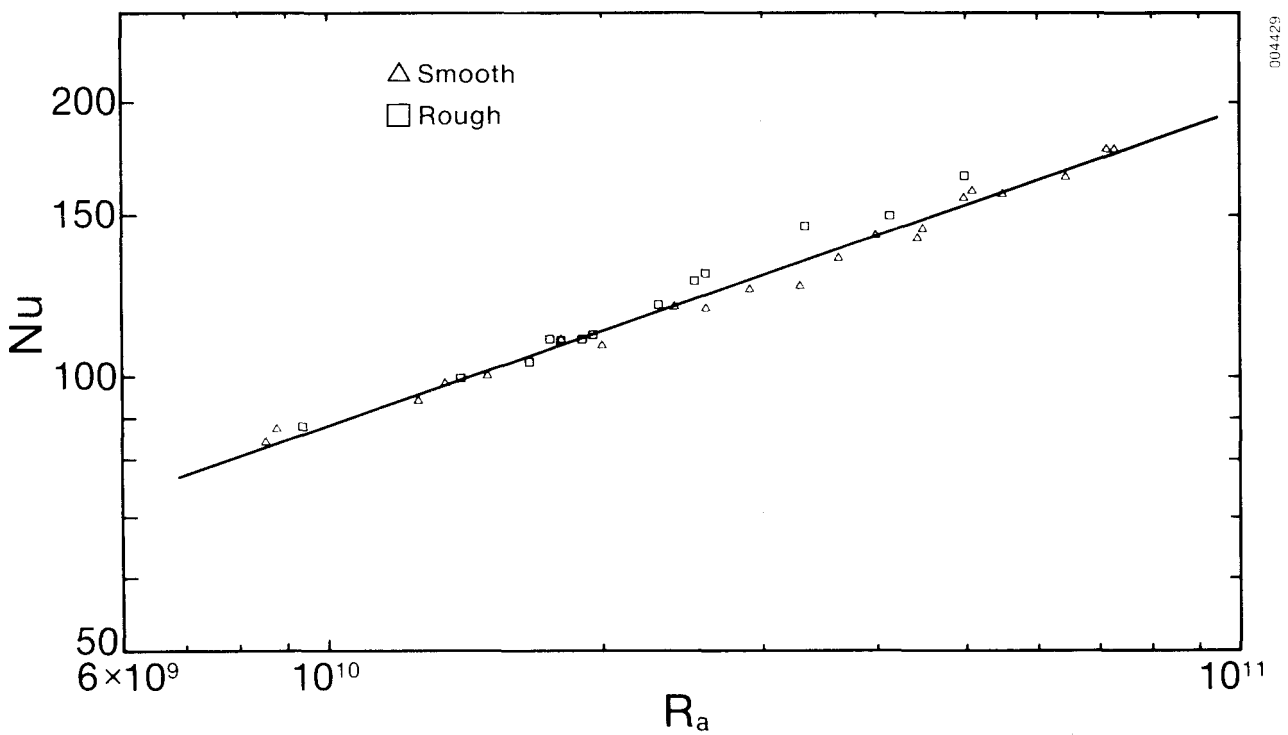

Figure 4-1. Average Nusselt Number for Isothermal Heated Plate

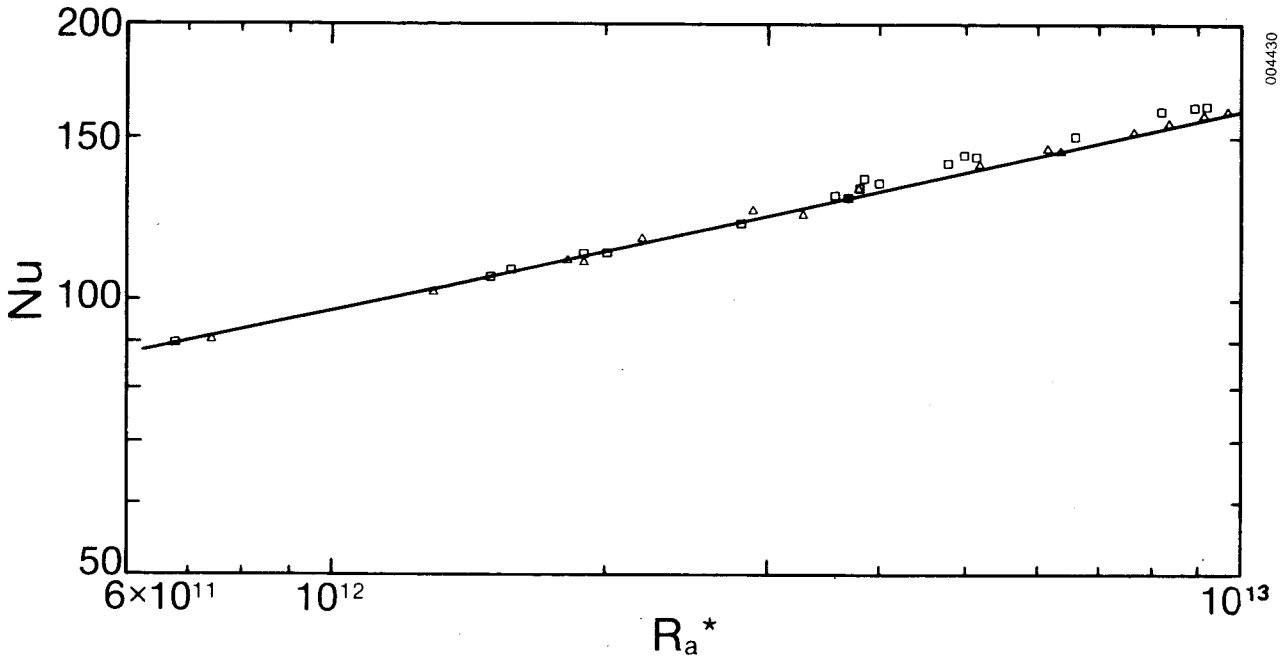

Figure 4-2. Average Nusselt Number for Constant Heat Flux Heated Plate

For the constant flux mode, Figure 4-2, one expects laminar data to follow a $Nu \sim Ra_*^{1/5}$ behavior. The rough data and smooth data are very close up to $Ra_* \sim 9 \times 10^{12}$ following this type of behavior. The obvious transition found in the isothermal case is not seen in the constant flux case. It is likely that transition occurs just outside the range, which could be attained with the existing apparatus; i.e., $Ra_* = 10^{13}$. The slight increase in heat transfer for the rough surface at the highest Ra_* could be the beginning of transition. Because of limitations on the maximum temperature for the heated wall, achieving a higher Ra_* will involve constructing a larger test cell. From Eq. 3-4, if the size of the test cell H were doubled, we could achieve $Ra_* = 3.2 \sim 10^{14}$, which should be sufficient to reveal transition.

Flow visualization photographs for the isothermal boundary condition are shown in Figures 4-3a,b, and c. Figure 4-3a is the rough surface at $Ra = 3.40 \times 10^{10}$, Figure 4-3b is the rough surface at $Ra = 1.40 \times 10^{10}$, and Figure 4-3c is the smooth surface at $Ra = 3.47 \times 10^{10}$. Referring to Figure 4-1, we see that these photographs correspond to conditions where the rough plate has assumed a behavior like $Nu \sim Ra^{1/3}$ but the smooth plate is still laminar, $Ra \cong 3.4 \times 10^{10}$ (Figures 4-3a,c). Figure 4-3b shows the rough plate at sufficiently low Rayleigh number so it is laminar.

Figure 4-3a shows transition occurring at approximately 5-6 cm from the bottom of the heated wall. The vertical grid lines are displaced smoothly to the right for heights from 0 to 5 or 6 cm from the bottom of the heated wall. Although displacement of the grid lines does not represent quantitatively the laminar boundary layer (which should be less than 1 mm thick at that point), it does give a good qualitative representation of where the boundary layer is steady (and the flow is essentially parallel to the wall) and where the flow begins to form waves and becomes unsteady; i.e., 5 or 6 cm from the bottom.

004436

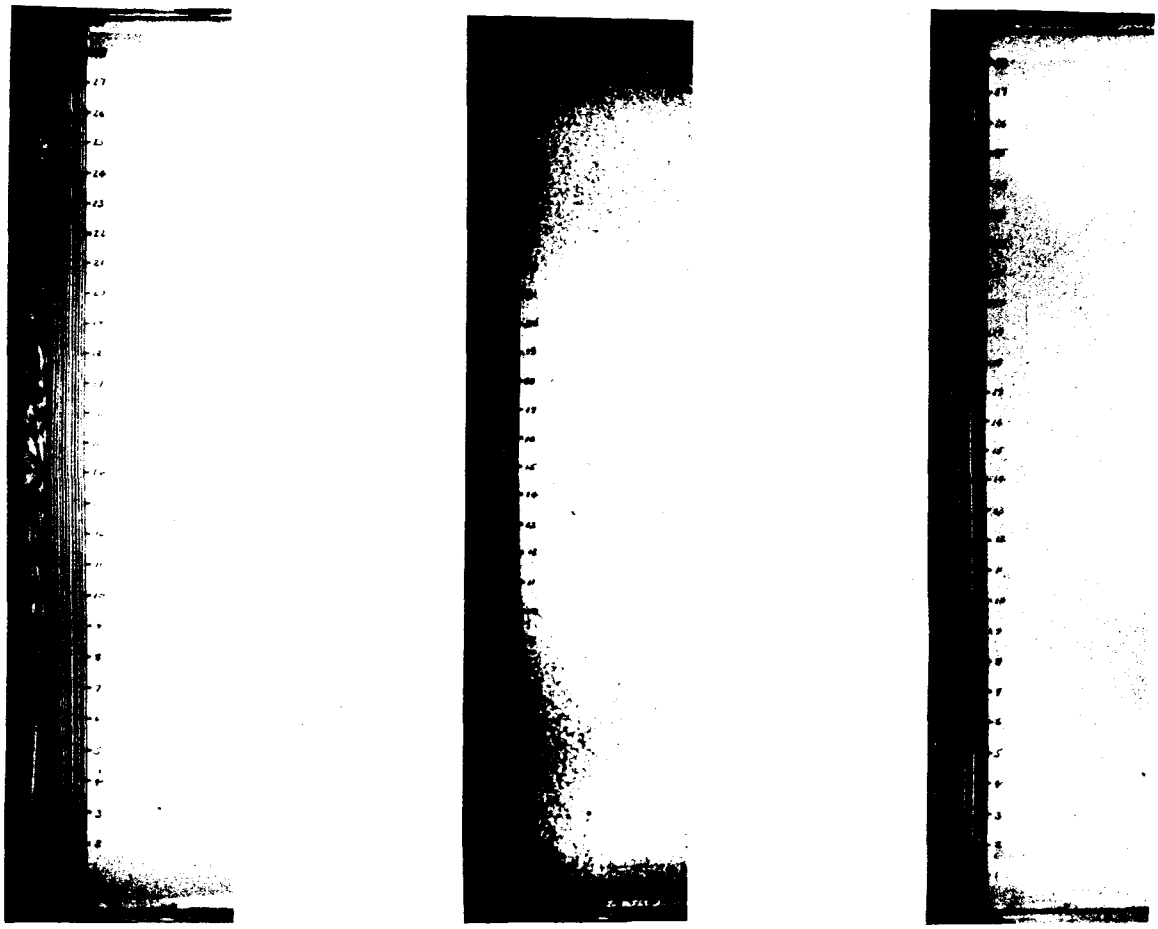

a. Rough Plate
$Ra = 3.40 \times 10^{10}$

b. Rough Plate
$Ra = 1.40 \times 10^{10}$

c. Smooth Plate
$Ra = 3.47 \times 10^{10}$

Figure 4-3. Flow Visualization

Above this height the unsteadiness becomes obvious, although the still photographs are not quite as descriptive as viewing in real time. The waviness in Figure 4-3a is first observed between 5 to 6 cm as a weak oscillation in the parallel grid lines. Between 6 to 7 cm, this oscillation becomes more pronounced until the waves begin to roll up between 8 to 9 cm. The waves continue to roll up until at approximately 13 to 14 cm the motion is very much a random one, indicating turbulent flow. Due to heater cycling, some variation in the height of initial waviness was observed. However, there was a very clear indication that the height for the rough plate was significantly less than that for the smooth plate.

Using the same flow visualization method for a vertical, heated cylinder in water and oil, Fujii et al. (1970) showed that the laminar boundary layer waviness first rolls up into pairs of counterrotating vortices. These vortices disintegrate, and transition then takes place. Because of the variation through the boundary layer (along a horizontal line parallel to the wall) in the present experiments, the light ray deflection results from an average effect. For a vertical cylinder it is possible to observe one small circumferential segment of the boundary layer at the cylinder tangent. The averaging effect in the present experiments does not allow one to see the formation, roll-up, and disintegration of the vortices.

At the lower Rayleigh number in Figure 4-3b, the rough plate exhibits similar behavior except, as expected, transition is delayed until considerably farther up the wall. In this case the initial oscillation of the grid lines appears near 10-11 cm, and the fully random motion occurs near 22-23 cm.

For the smooth surface at $Ra = 3.47 \times 10^{10}$, Figure 4-3c, the boundary layer appears laminar up to 14-15 cm where unsteadiness is first observed. Random motion is observed near 24-25 cm, much higher than on the rough plate at the same Rayleigh number. Thus, in agreement with the heat transfer data, Figure 4-1, the roughness causes the laminar boundary layer to undergo transition to turbulence earlier than on the smooth plate. The rough plate exhibits a boundary layer that is turbulent over a much greater extent of the heated plate. Since the turbulence increases heat transfer locally, the rough plate exhibits higher average heat transfer as shown in Figure 4-1.

A comparison of the local heat transfer from the rough and smooth plates is made in Figures 4-4a,b, and c. The data displayed in these figures covers the range $Ra = 1.9 \times 10^{10}$ to $Ra = 4.1 \times 10^{10}$ and represents the average heat transfer from a horizontal strip centered on the x-location shown on the figures. Each horizontal strip is composed of four of the 16 heaters used to control the temperature of the plate. The experimental error associated with these results is $\approx \pm 7\%$. The solid line in the figures is based on a correlation provided by Schinkel (1983) in the laminar regime for $A \geq 4$, $Pr = 0.7$, and $10^5 \leq Ra/A^3 \leq 4 \times 10^5$. Figure 4-4a is for a Ra at which no enhancement in the average Nu occurs and indicates that there is little effect upon the local Nu, except perhaps in the upper corner. Figures 4-4b and c are for Ra for which the average Nu is increased by the presence of the rough plate. They indicate that this effect is a result of a dramatic (~40%) increase in local heat transfer near $x = 0.6 \times H$. The highest locations in Figures 4b and c do not exhibit any increase in local heat transfer even though the point immediately below that location does. This appears to be related to detrainment of fluid from the boundary layer near the top of the enclosure, which reduces the mixing effect roughness of the elements, as discussed in Section 2.1.

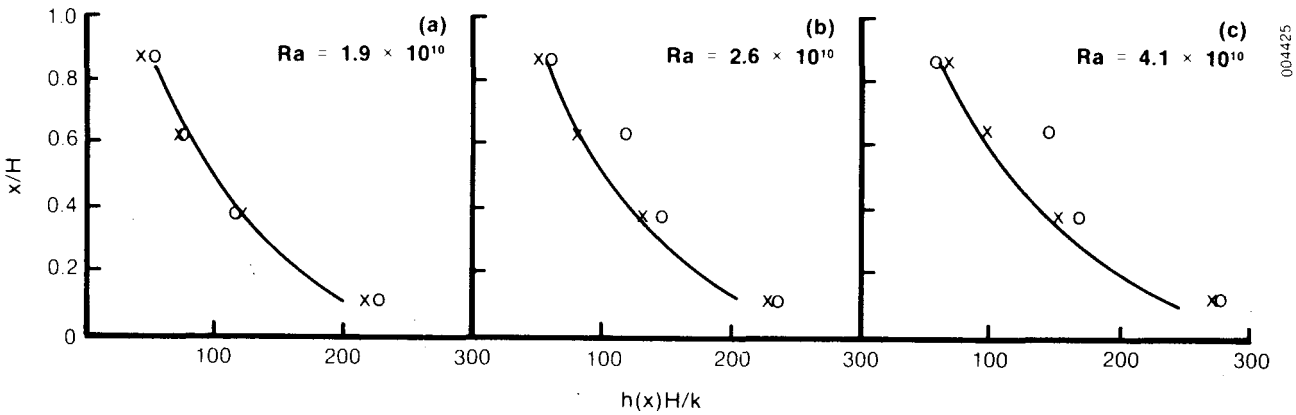

Figure 4-4. Local Heat Transfer Data

SECTION 5.0

CONCLUSIONS AND RECOMMENDATIONS

A review of the literature revealed very little information on the enhancement of natural convection and none specific to that in enclosures. In the literature available on natural convection enhancement there is conflicting evidence regarding the possibility of increasing convective heat transfer coefficients by modifying the nature of the heat transfer surface.

In this study it was shown conclusively that it is possible to significantly increase heat transfer coefficients in that manner. One vertical heated wall of an enclosure was machined in such a way that protrusions, 1 mm square with 1-mm spacing, resulted. Based on previous analytical solutions for the natural flow up a heated vertical plate in an infinite medium, this protrusion height is the same order as the boundary layer thickness.

Comparing dimensionless average heat transfer coefficients (Nusselt number) for the rough plate and a smooth plate, which was also tested in this study, the most noticeable difference occurred in the transition regime. The roughened plate began to exhibit turbulent behavior at a Ra approximately half that of the smooth plate. In this regime, the average Nu for the rough plate are about 16% greater than for the smooth plate.

Flow visualization studies indicate that the roughness promotes the transition to turbulence. At $Ra = 3.4 \times 10^{10}$ the rough plate exhibited a turbulent boundary layer over approximately 81% of the plate while the smooth plate at the same Ra exhibited a laminar boundary layer over approximately 50% of the plate. Local increases in heat transfer coefficient of approximately 40% were observed.

There appears to be no enhancement effect in the laminar regime, $Ra < 2 \times 10^{10}$, but a slight enhancement effect was seen in the turbulent regime, $Ra > 5 \times 10^{10}$. It would appear that this type of rough surface is most effective in promoting transition.

The present work provides proof of concept and clarifies some of the inconsistencies from previous work in the literature. Although the single rough surface tested did not produce very large increases in average heat transfer, it did demonstrate the potential for natural convection enhancement. Many other types of surface roughness have been tested for forced convection enhancement and should be considered for natural convection enhancement. These include sand-grain random roughness, repeated transverse ribs, and isolated boundary layer trips to promote transition.

Isolated boundary layer trips can promote transition to turbulence, but as shown for forced flow, the trip must be a certain height to destabilize the boundary layer. If the trip is too small, a recirculating flow may be established behind the trip, but the flow will reattach beyond this point and resume laminar flow. Increases in heat and mass transfer do occur near the reattachment point providing a possible mechanism for overall enhancement; i.e., repeated trips. On the other hand, a better understanding of the

boundary layer flow, especially considering factors unique to enclosures such as the corners and stratification, is necessary to redefine the minimum isolated trip size for natural flows. Otherwise, we must rely on previous work for forced flow.

In the turbulent regime, manipulation of the viscous sublayer, i.e., improved mixing by small roughness elements, will increase the heat transfer beyond the transition point. For natural flow an important question is whether too large a roughness impedes the bouyant forces and thus offsets any gains in heat transfer. If so, one must determine the size of roughness that yields the greatest local heat transfer.

A better understanding of the interaction of naturally driven flows with surface roughness is needed to allow one to provide the maximum heat transfer for a given application. This requires a detailed investigation of the boundary layer interaction with different roughness elements. This investigation would provide local temperature, velocity, and heat flux data. These local measurements, especially near isolated roughness elements, would help explain the mechanisms of boundary layer interaction with surface roughness. The data shown in Figure 2-4 for turbulence promoters in forced flow mass transfer are typical of the data needed for natural convection flow. There, a combination of flow visualization and local mass transfer measurements shows how the turbulence promoter modified the channel flow resulting in a subsequent increase in mass transfer.

A detailed investigation, such as the one for natural convection, could reveal how to trip the boundary layer into turbulence as early as possible and then how to increase heat transfer in the turbulent regime.

SECTION 6.0

REFERENCES

Bergles, A. E., 1978, "Enhancement of Heat Transfer," Proceedings of the 6th International Heat Transfer Conference, Vol. 6, Washington, DC: Hemisphere Publishing Co.

Bohn, M. S., D. A. Olson, and A. T. Kirkpatrick, 1983, "Experimental Study of Three-Dimensional Natural Convection at High Rayleigh Number," ASME/JSME Thermal Engineering Joint Conference Proceedings-Vol. 1, accepted for publication, ASME J. Heat Transfer.

Dipprey, D. F., and R. H. Sabersky, 1963, "Heat and Momentum Transfer in Smooth and Rough Tubes at Various Prandtl Numbers," Int. J. Heat Mass Transfer, Vol. 6, pp. 329-353.

Fujii, T., M. Takeuchi, K. Suzaki, and H. Uehara, 1970, "Experiments on Natural Convection Heat Transfer from the Outer Surface of a Vertical Cylinder to Liquids," Int. J. Heat Mass Transfer, Vol. 13, pp. 753-787.

Fujii, T., M. Fujii, and M. Takeuchi, 1973, "Influence of Various Surface Roughness on the Natural Convection," Int. J. Heat Mass Transfer, Vol. 16, pp. 629-640.

George, W. K., and S. Capp, 1979, "A Theory for Natural Convection Turbulent Boundary Layers Next to Heated Vertical Surfaces," Int. J. Heat Mass Transfer, Vol. 22, pp. 813-826.

Heya, N., M. Takeuchi, and T. Fujii, 1982, "Influence of Surface Roughness on Free-Convection Heat Transfer from a Horizontal Cylinder," The Chemical Engineering Journal, Vol. 23, pp. 185-192.

Joffre, L. J., and R. F. Barron, 1967, "Free-Convection Heat Transfer to a Rough Plate," Paper No. 67-WA/HT-38, American Society of Mechanical Engineers.

Kang, I. S., and H. N. Chang, 1982, "The Effect of Turbulence Promoter on Mass Transfer--Numerical Analysis and Flow Visualization," Int. J. Heat Mass Transfer, Vol. 25, pp. 1167-1181.

Lewis, M. J., 1975, "An Elementary Analysis for Predicting Momentum and Heat-Transfer Characteristics of a Hydraulically Rough Surface," J. Heat Transfer, Vol. 97, pp. 249-254.

Nakayama, W., 1982, "Enhancement of Heat Transfer," Vol. 1, Proceedings of the 7th International Heat Transfer Conference, Washington, DC: Hemisphere Publishing Co.

Neeper, D. A., and R. D. McFarland, 1982, "Some Potential Benefits of Fundamental Research for the Passive Solar Heating and Cooling of Buildings," LA9425-MS, Los Alamos, NM: Los Alamos National Laboratory.

Prasolov, R. S., 1961, "On the Effects of Surface Roughness in Natural-Convection Heat Transfer from Horizontal Cylinders to Air," Inzh. Fiz. Zh. Vol. 4, pp. 3-7.

Raithby, G. D., and K. G. T. Hollands, 1975, "A General Method of Obtaining Approximate Solutions for Laminar and Turbulent Free Convection Problems," Advances in Heat Transfer, Vol. II, Academic Press, pp. 265-315.

Sabersky, R. H., A. J. Acosta, and E. G. Hauptmann, 1971, Fluid Flow, 2nd Edition, New York: The MacMillan Co.

Sastry, C. V. N., V. N. Murthy, and P. K. Sarma, 1976, "Effect of Discrete Wall Roughness on Free Convective Heat Transfer from a Vertical Tube," Heat Transfer and Turbulent Bouyant Convection, Vol. 2, Washington, DC: Hemisphere Publishing Co.

Schinkel, W. M. M., S. J. M. Linthorst, and C. J. Hoogendoorn, 1983, "The Stratification in Natural Convection in Vertical Enclosures," J. of Heat Transfer, Vol. 105, pp. 267-272.

Schlicting, H., 1968, Boundary-Layer Theory, 6th Edition, New York: McGraw-Hill.

Seban, R. A., and Caldwell, G. L., 1968, "The Effect of a Spherical Protuberence on the Local Heat Transfer to a Turbulent Boundary Layer," J. Heat Transfer, Vol. 90, pp. 408-412.

Vliet, G. C., and C. K. Liu, 1969, "An Experimental Study of Turbulent Natural Convection Boundary Layers," J. Heat Transfer, Vol. 91, pp. 517-531.

Webb, R. L., 1979, "Toward a Common Understanding of the Performance and Selection of Roughness for Forced Convection," Studies in Heat Transfer, J. P. Hartnet et al., eds., Washington, DC: Hemisphere Publishing Co.

Webb, R. L., 1980, "Special Surface Geometries for Heat Transfer Augmentation," Development in Heat Exchanger Technology--1, D. Chisolm, ed., Essex, England: Applied Science Publishers, Ltd.

Webb, R. L., and A. E. Bergles, 1983, "Heat Transfer Enhancement: Second Generation Technology," Mechanical Engineering, June, pp. 60-67.

APPENDIX A

BOUNDARY LAYER EQUATIONS

This appendix provides several equations that describe flow in a boundary layer. Detailed derivations of each relationship are available in Schlicting (1968) and Sabersky et al. (1971).

The equations of motion for laminar flow over a flat plate parallel to the flow (the Blasius problem) may be solved exactly or by approximate techniques such as the integral method. The velocity profile is given in Figure A-1 in the dimensionless form:

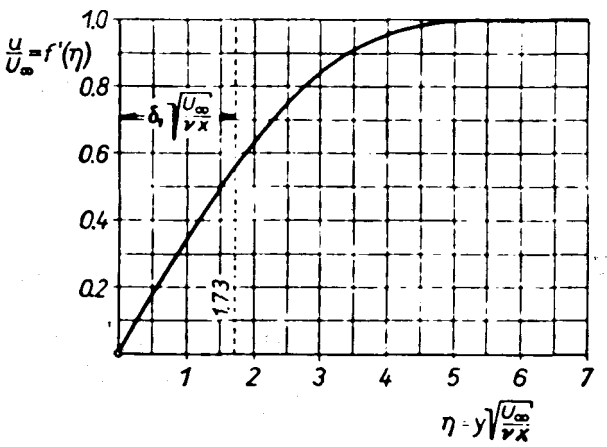

(a) Velocity distribution in the boundary layer along a flat plate

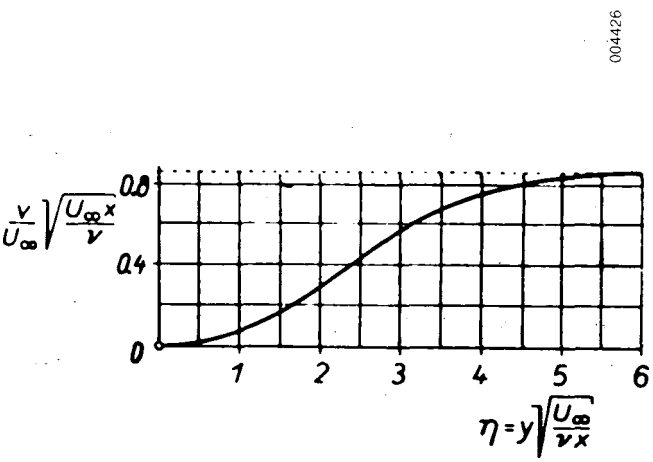

(b) The transverse velocity component in the boundary layer along a flat plate

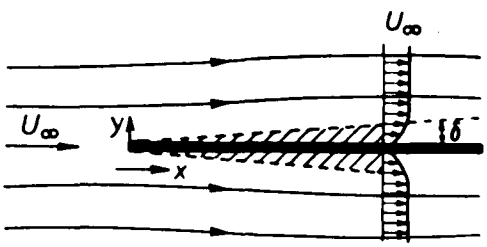

(c) The boundary layer along a flat plate at zero incidence

Figure A-1. Solution of the Blasius Problem
Source: Schlicting (1968)

$$u/U_\infty = f\left[y\ (U_\infty/\nu x)^{1/2}\right] , \tag{A-1}$$

and the symbols are also defined in the same figure.

The local shearing stress is given by

$$\tau_o\ (x) = 0.332\ \rho U_\infty^{\ 2}\ Re_x^{-1/2} , \tag{A-2}$$

where

$$Re_x = U_\infty x/\nu .$$

The boundary layer thickness defined as the distance y in Eq. A-1 for which $u/U_\infty = 0.99$ is

$$\delta \sim 5\ Re_x^{-1/2} . \tag{A-3}$$

In turbulent flow the (mean) velocity profile is given in terms of the so-called law-of-the-wall:

$$\frac{u}{u_*} = 5.75\ \log\left(\frac{yu_*}{\nu}\right) + 5.5 \text{ for } yu_*/\nu > 30 \tag{A-4}$$

and

$$\frac{u}{u_*} = \frac{yu_*}{\nu} \text{ for } yu_*/\nu < 5 . \tag{A-5}$$

The friction velocity is given by $u_* = (\tau_o/\rho)^{1/2}$.

Equation A-4 may be approximated by

$$\frac{u}{u_*} = 8.7\ \left(\frac{yu_*}{\nu}\right)^{1/7} . \tag{A-6}$$

Equation A-4 for $yu_*/\nu > 30$ is the velocity profile in the turbulent core, while Eq. A-5 for $yu_*/\nu < 5$ is for the viscous sublayer. Velocity in the transition region, $5 < yu_*/\nu < 30$, follows a smooth curve between Eqs. A-4 or A-5 and A-6, see Figure A-2. The local shearing stress at the wall is

$$\tau_o(x) = 0.0465\ \rho U_\infty^2\ (\alpha/Re_x)^{1/5} , \tag{A-7}$$

where

$$Re_x = U_\infty\ x/\nu$$

and

$$\alpha = \int_0^1 \left(1 - \frac{u}{U_\infty}\right)\left(\frac{u}{U_\infty}\right)\ d\left(\frac{y}{\delta}\right) .$$

For turbulent flow over a rough surface, Eq. A-4 is valid if the constant 5.5 is replaced by a function of $\varepsilon_s u_*/\nu$, which has the value 8.5 for $\varepsilon_s u_*/\nu > 2$.

For laminar natural convection flow up (down) a heated (cooled) vertical plate the velocity distribution is given in Figure A-3 with

$$\frac{u}{2\sqrt{gx}}\sqrt{\frac{T_\infty}{T_\omega - T_\infty}} = f\left[\frac{y}{x}\ \left(\frac{Gr_x}{4}\right)^{1/4}\right] . \tag{A-8}$$

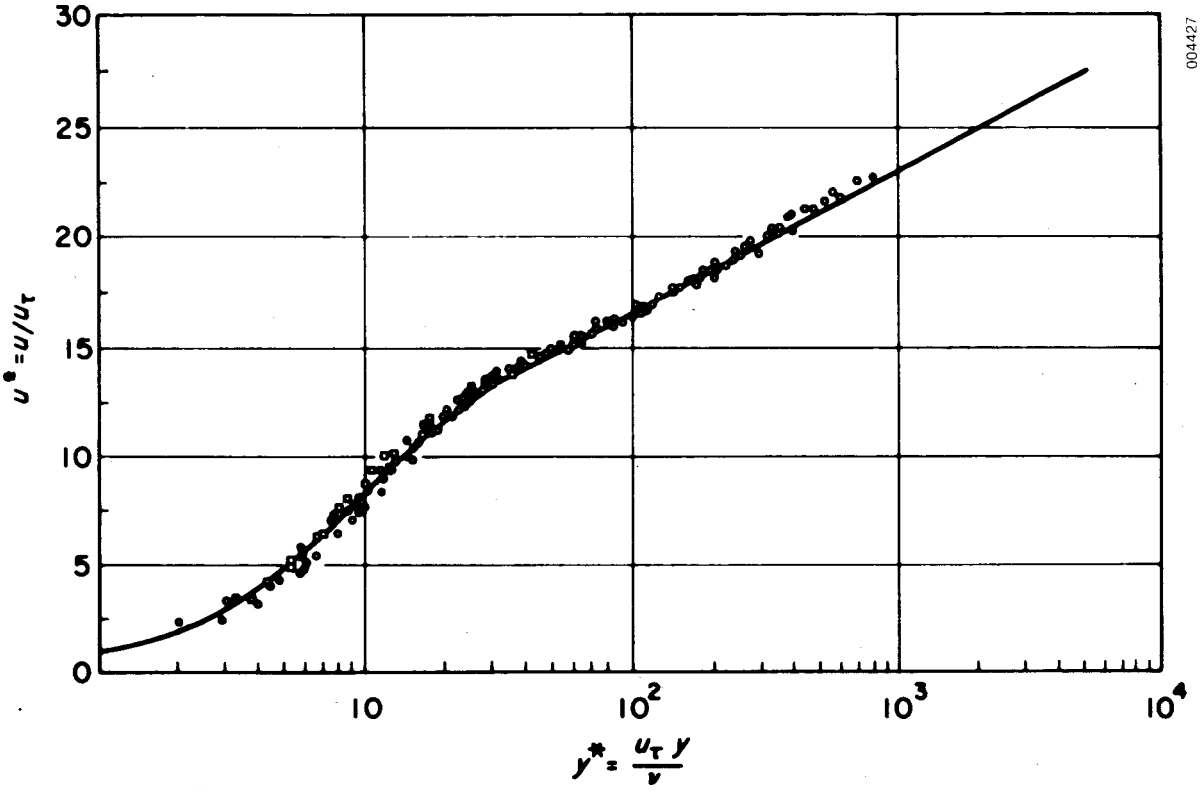

Dimensionless velocity profile u^* vs. y^*. This type of representation could have been expected for the region near the wall. It actually gives a fair representation even at distances where r/r_o differs significantly from unity. In addition the profile for the flow near a flat plate is also well approximated by the graph in the figure. This velocity profile has, therefore, often been called a universal one.

Figure A-2. Velocity Profile for Turbulent Flow over a Flat Plate
Source: Sabersky et al. (1971)

Vliet and Liu (1969) measured velocity and temperature profiles near a heated vertical flat plate with a turbulent boundary layer. They recommended an equation like Eq. A-6 with a multiplying factor to allow the velocity to become zero at the edge of the boundary layer:

$$\frac{u}{U_{max}} = 1.87\left(\frac{y}{\delta}\right)^{1/10}\left(1 - \frac{y}{\delta}\right)^4 . \qquad \text{(A-9)}$$

Their data was best fit by

$$\frac{u}{U_{max}} = 1.61\left(\frac{y}{4.1\delta*}\right)^{1/10}\left(1 - \frac{y}{4.1\delta*}\right)^4 \text{ for } y/\delta* > 0.15 , \qquad \text{(A-10)}$$

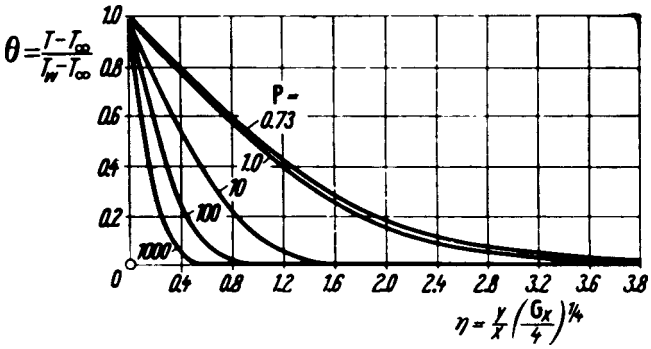

Temperature distribution in the laminar boundary layer on a hot vertical flat plate in natural convection. Theoretical curves, for P = 0·73

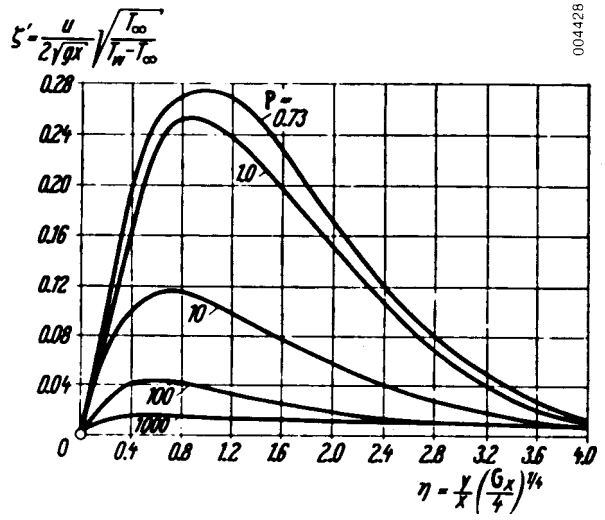

Velocity distribution in the laminar boundary layer on a hot vertical flat plate in natural convection

Figure A-3. Velocity Profile for Laminar Natural Convection up a Vertical Heated Plate
Source: Schlicting (1968)

where δ_* is the displacement thickness $\delta_* = \int_0^\infty u/U_{max}\, dy$.

They recommended for the friction velocity

$$u_{1*} = \frac{\nu}{x} Gr_x^{1/2} \qquad \text{(A-11)}$$

or

$$u_{3*} = \frac{\nu}{x} Ra_x^{1/2} \qquad \text{(A-12)}$$

to account for Pr effects. However, they did not find that plotting the velocity against a function of yu_*/ν improved the similarity found by Eq. A-10.

George et al. (1979) used a method closely related to Raithby and Hollands' (1974) conduction layer model to develop the velocity and temperature profile for turbulent natural convection flow on vertical plate. For the region near the wall they found a result identical to Eq. A-5.

The form of the velocity profiles recommended by Vliet and Liu (1969) and others is based on forced convection profiles, i.e, the law of the wall, and was modified for the special behavior of the natural convection boundary layer, which has zero velocity at the wall and far away from the wall. According to Vliet and Liu (1969), the procedure is well accepted for natural-convection, turbulent, boundary-layer analysis.

DISTRIBUTION

Prof. R. I. Loehrke
Department of Mechanical Engineering
Colorado State University
Ft. Collins, CO 80523

Prof Allan Kirkpatrick
Department of Mechanical Engineering
Colorado State University
Ft. Collins, CO 80523

Prof. O. A. Plumb
College of Engineering
Washington State University
Pullman, WA 99164-2714

R. W. Jones
Los Alamos National Laboratory
Los Alamos, NM 87545

K. Yamaguchi
Los Alamos National Laboratory
Los Alamos, NM 87545

Fred Bauman
Passive Solar Analysis & Design Group
Lawrence Berkeley Laboratory
University of California
Berkeley, CA 94720

Professor Arthur Bergles
Department of Mechanical Engineering
Iowa State University
Ames, IA 50010

Professor Benjamin Gebhart
Department of Mechanical Engineering
and Applied Mechanics
University of Pennsylvania
Philadelphia, PA 19104